



# Robust Predictors for Seasonal Atlantic Hurricane Activity Identified with Causal Effect Networks

Peter Pfleiderer<sup>1,2,3\*</sup>, Carl-Friedrich Schlessner<sup>1,2,3</sup>, Tobias Geiger<sup>3,4</sup>, Marlene Kretschmer<sup>5</sup>

5 <sup>1</sup> Climate Analytics, Berlin, Germany

<sup>2</sup> IRI THESys, Humboldt Universität Berlin, Berlin, Germany

<sup>3</sup> Potsdam Institute for Climate Impact Research, Potsdam, Germany

<sup>4</sup> German Meteorological Service, Climate and Environment Consultancy, Stahnsdorf, Germany

<sup>5</sup> University of Reading, Department of Meteorology, Reading, UK

10 *Correspondence to:* Peter Pfleiderer (peter.pfleiderer@climateanalytics.org)

**Abstract.** Atlantic hurricane activity varies substantially from year to year and so do the associated damages. Longer-term forecasting of hurricane risks is a key element to reduce damages and societal vulnerabilities by enabling targeted disaster preparedness and risk reduction measures. While the immediate synoptic drivers of tropical cyclone formation and intensification are increasingly well understood, precursors of hurricane activity on longer time-horizons are still not well established. Here we use a causal network-based algorithm to identify physically motivated late-spring precursors of seasonal Atlantic hurricane activity. Based on these precursors we construct seasonal forecast models with competitive skill compared to operational forecasts. We present a skillful model to forecast July to October cyclone activity at the beginning of April. Earlier seasonal hurricane forecasting provides a multi-month lead time to implement more effective disaster risk reduction measures. Our approach also highlights the potential of applying causal effects network analysis in seasonal forecasting.

## 20 **1 Introduction**

Tropical cyclones (TCs) are among the most damaging weather events in many tropical and subtropical regions. The compound nature of tropical cyclone hazards combining heavy winds, extreme precipitation and coastal flooding contributes to their severity (Ye and Fang 2018), directly impacting societies. Furthermore, a range of secondary impacts in the aftermaths of cyclones such as displacement, loss in livelihoods or income, and health impacts are being reported (Camargo and Hsiang 2014). Applying risk reduction measures to the direct damages of TCs is challenging and is expected to become even more so with global warming and sea level rise (Woodruff et al. 2013). Preparedness for the secondary impacts can however be improved if reliable forecasts for the potential risks of the upcoming hurricane season are available (Martinez 2018).

Several institutes provide seasonal hurricane forecasts for the Atlantic basin (Klotzbach 2019). The Colorado state university was one of the first institutes already issuing seasonal forecasts in 1984 (Gray 1984a, b). A whole variety of forecasting methods are applied ranging from purely statistical forecasts to forecasts based on regional climate model simulations and hybrid approaches (Klotzbach et al. 2017; Klotzbach 2019).



Dynamical forecast models are based on global or regional circulation models that simulate the climate including tropical cyclone occurrences (Vitart and Stockdale 2001; Vecchi et al. 2014; Manganello et al. 2017). Their skill depends on their ability to represent TC genesis and development and their capacity to forecast the large-scale circulation over the Atlantic main development region (MDR). With increasing spatial resolution their representation of TCs improves. Their ability to predict the large-scale circulation and low frequency variability can, however, remain a limiting factor for seasonal forecasts (Manganello et al. 2017).

Statistical forecast models are usually based on favorable climatic conditions in the region of TC formation and established teleconnections affecting cyclone activity on the basins scale (Klotzbach et al. 2017). Besides warm sea surface temperatures (SST), both the formation and intensification of TCs critically depend on low vertical wind shear (VWS) over the tropical Atlantic (Frank and Ritchie 2001; Emanuel et al. 2004). Furthermore, dry air intrusion and anticyclonic wave breaking can hamper TC formation (Hankes and Marinaro 2016). Finally, a lack of easterly African waves can lead to lower TC activity (Dieng et al. 2017; Patricola et al. 2018).

Classical statistical forecast models are often based on correlation analysis and expert judgement with regard to the inclusion of potential predictors in the model. One major challenge in statistical forecasting is yet to select a set of skillful predictors without running into overfitting issues, resulting in dropping skill when applied to independent test data (Hawkins 2004).

Recently, a novel statistical forecast approach based on causal effect networks (CEN) emerged (Kretschmer et al. 2017; Di Capua et al. 2019; Saggioro and Shepherd 2019). In such a network, including the predictand and a set of potential predictors detected from gridded climate data, causal links are identified by iteratively testing for conditionally independent relationships, thereby removing spurious correlations (Runge et al. 2019b). First applications have shown that statistical forecast models based on causal precursors result in skillful forecasts as they identify relevant predictors without overfitting (Kretschmer et al. 2017; Di Capua et al. 2019).

Here we apply this approach to explore remote climate predictors in spring of hurricane activity from July to October. We first demonstrate the applicability of the method by constructing a forecast for the July-October accumulated cyclone energy (ACE) based on May reanalysis. The identified precursors are well documented drivers of hurricane activity in the Atlantic. To increase forecast lead time, we then apply the same method to construct a forecast based on March reanalysis and obtain competitive forecast skill based on these novel predictors.



## 2 Methods

### 60 2.1 Data

Tropical cyclone locations and maximum sustained wind speeds from the official WMO agency are taken from the IBTrACS database (Knapp et al. 2010, 2018).

The main analysis is based on the fifth generation of ECMWF atmospheric reanalyses (ERA5) (Copernicus Climate Change Service (C3S) 2017). We use the monthly reanalysis data provided on a regular 1-degree grid. For sensitivity testing, we also  
65 use the Japanese 55-year reanalysis (JRA55) provided on monthly time-scale and on a regular 1.25-degree grid (The Japan Meteorological Agency (JMA) 2013).

### 2.2 Accumulated Cyclone Energy (ACE)

Following Waple et al. (2002), we calculate accumulated cyclone energy (ACE) as an indicator for seasonal tropical cyclone  
70 activity:

$$ACE = 10^{-4} \sum_{all\ days} v_{max}^2, \quad (1)$$

ACE is accumulated for TCs within the Atlantic basin with maximal sustained wind speeds above 34knots and all days in July-October.

### 75 2.3 Causal effect networks (CEN)

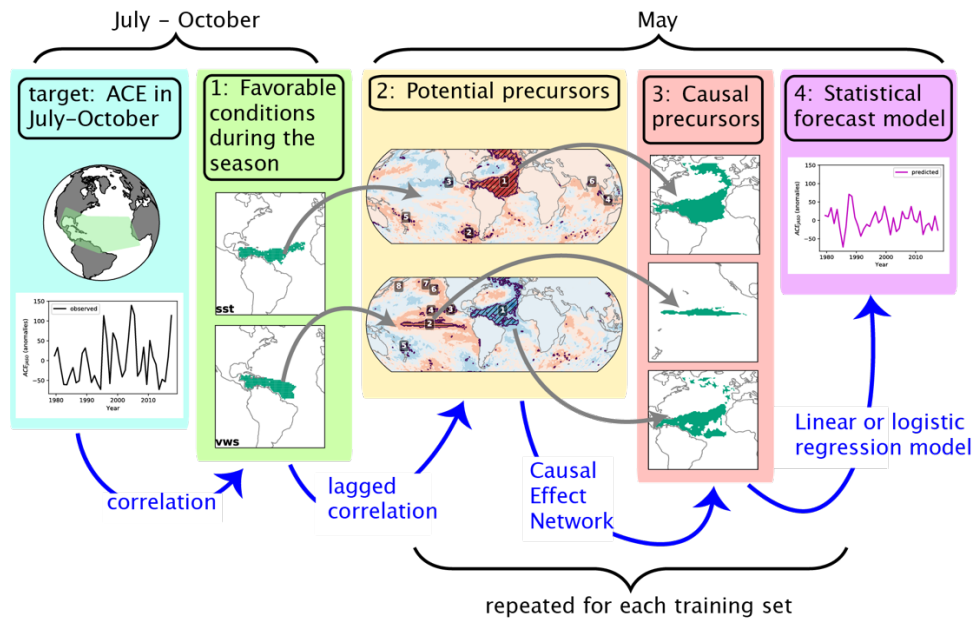
Causal effect networks have been introduced to statistically analyze and visualize causal relationships between different climatic processes, referred to as “actors”. Specifically, spurious correlations due to indirect links, common drivers or autocorrelation effects are identified as such and removed from the network structure (Kretschmer et al. 2016; Runge et al. 2019b). The remaining links can then be interpreted in a more causal way within the set of considered variables.

80 Here we use a two-step approach to construct causal effect networks consisting of a condition selection algorithm (PC-algorithm) and a momentary conditional independence (MCI) test. This so called PCMCI algorithm was implemented by Jakob Runge and is openly available on [github.com/jakobrunge/tigramite](https://github.com/jakobrunge/tigramite) (Runge 2014). The properties of the PCMCI algorithm are documented and discussed in Runge et al. (2019).

Note that this algorithm requires several preconditions to be met (Runge 2018). Specifically, it requires a comprehensive  
85 sampling of potentially relevant climate signals as well as sufficient temporal coverage to ensure full representation of multi-annual to multi-decadal modes. Only such a comprehensive coverage can allow for the identification of all spurious links and causal pathways. The condition of full climate signal coverage is not strictly fulfilled in our application of seasonal forecasting as we only select climate variables within a fixed time lag. As such, we cannot exclude potential common drivers on longer, e.g. annual time scales. For our application in seasonal forecasting, potentially existing common drivers do not represent a  
90 problem. However, this represents a divergence from the original methodological approach of causal precursor analysis.



Therefore, we will refer to the results of the CEN analysis as “robust precursors” acknowledging that we cannot assure *full true* causality here.



95

**Figure 1: Forecast model construction.** Four steps are performed to build a forecast model for ACE in July-October (left): 1) Regions of interest for two favourable conditions of hurricane activity (SST and VWS) are identified. 2) For each of the favourable conditions of 1) potential precursors in May are identified by clustering the most significantly correlated grid cells within SST data. 3) Causal effect networks are used to select a small set of robust precursors. 4) A statistical model is build based on the identified robust precursors of 3). Steps 2)-4) are repeated for the different training sets leading to a different forecast model for each predicted year.

100

## 2.4 Using CEN as a robust precursor selection tool in a forecast model

We apply a CEN approach to identify robust precursors in May (and in March) for hurricane season activity the same year.

105

Similar to Kretschmer et al. (2017), our methodology consists of 4 steps (visualized in Fig. 1):

1. We identify regions where **favourable conditions for TC** formation and intensification are most relevant. Here we use SSTs and VWS fields as established favourable conditions but without prescribing spatial patterns. We then identify regions in the Atlantic that are correlated with ACE during the hurricane season (July to October) (see Fig. 2).
- 110 2. We search for **potential precursors of the favourable conditions** identified in step 1. For this we calculate lagged point correlation maps with gridded SST or mean sea level pressure (MSLP) data and cluster the most significantly correlated points into potential precursor regions.
3. We identify **robust precursors** amongst all potential precursor regions identified in step 2 by applying the CEN algorithm PCMCI.



- 115 4. We construct a **statistical forecast model** based on the robust precursors identified in step 3. While for the  
detection of potential and robust precursors (step 2 & 3) detrended anomalies of climate variables are used, the final  
forecast models are constructed with the raw reanalysis data.

More details including all relevant significance thresholds and clustering parameters are listed and discussed in the SI.

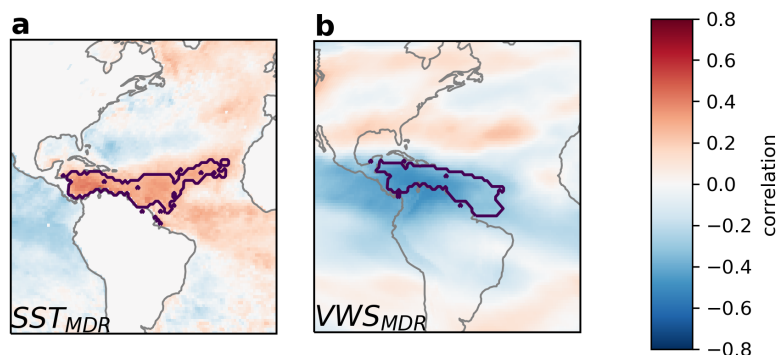
## 120 2.5 Forecast model evaluation

We evaluate the skill of our forecast model by performing a cross-validation prediction: For each predicted year, we construct  
a new forecast model using all years but the year we want to predict as well as the two preceding years. Specifically, steps 2-  
4 are iteratively performed for each predicted year (see Fig. 1). By excluding the two preceding years from the training set, we  
assure that autocorrelations of up to 3 years do not leak information from the training data into the testing data.

- 125 As recently discusses by Li et al. (2020), such cross-validation tests do not assure the reproducibility of the forecast skill in  
the real world. For the sake of readability, we will still refer to our cross-validated predictions as “forecasts”. And in distinction  
to that we will refer to forecasts that have been tested in the real world as “operational forecasts”.

## 3 Results

- Favorable conditions** for active hurricane seasons are (among others) warm SSTs and low VWS over the western tropical  
130 North Atlantic (Fig. 2). We identify the regions where the association of SSTs and VWS on basin wide ACE is strongest by  
clustering most strongly correlated grid-cells (see SI for more information). These regions cover large parts of the main  
development region (MDR) and we call them  $SST_{MDR}$  and  $VWS_{MDR}$ . The relationships between these variables and TC  
formation as well as TC intensification are well documented (Frank and Ritchie 2001).



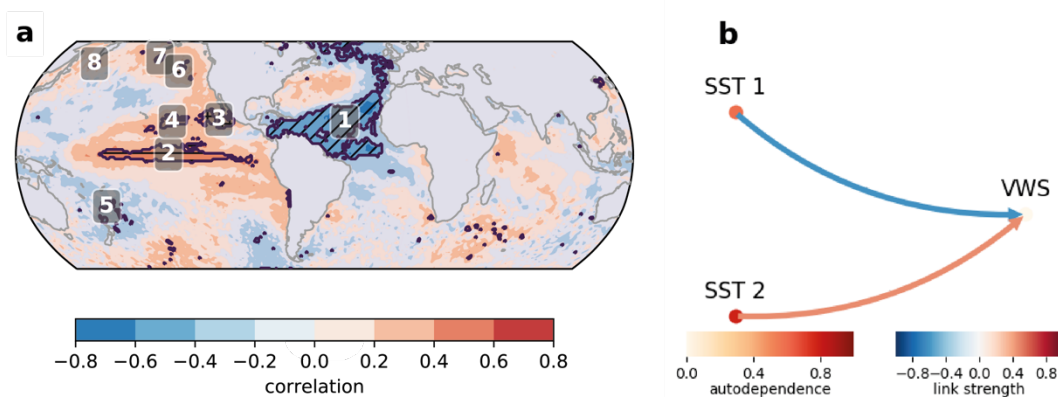
135

**Figure 2: Favorable conditions for high ACE in July-October. a: Point correlation between SST and basin wide mean ACE in July-October. The contour line indicates the identified region in the Atlantic basin. b: As (a) but for VWS. Details on the definition of the region are described in the supplementary information.**



140 To identify **potential precursors** (step 2 in Fig. 1) of  $SST_{MDR}$  and  $VWS_{MDR}$  we calculate lagged point correlation maps between the regional averages of  $VWS_{MDR}$  ( $SST_{MDR}$ ) and gridded SST data.  $VWS_{MDR}$  in July-October is strongly correlated with SSTs in May in several locations. Potential precursor regions are found in the tropical Atlantic and Pacific, in the northern North Atlantic and in the northeastern Pacific (see Fig. 3a).

We then construct a **causal effect network** (step 3 in Fig. 1) with all identified potential precursors. We find that warm SSTs in the tropical Pacific and cold SSTs in the subtropical North Atlantic are *robust* precursors of strong  $VWS_{MDR}$  (Fig. 3b). The signal from the Pacific resembles the Niño3.4 region and thus reflects the El Niño Southern Oscillation (ENSO) which is a well-known driver of variations in hurricane activity (Gray 1984a; Tang and Neelin 2004; Kim et al. 2009). In combination, the difference between tropical Atlantic SSTs and Pacific SSTs is consistent with the hypothesis that Atlantic hurricane activity mainly depends on the temperature of Atlantic SSTs relative to the other basins (Vecchi and Soden 2007; Murakami et al. 2018).

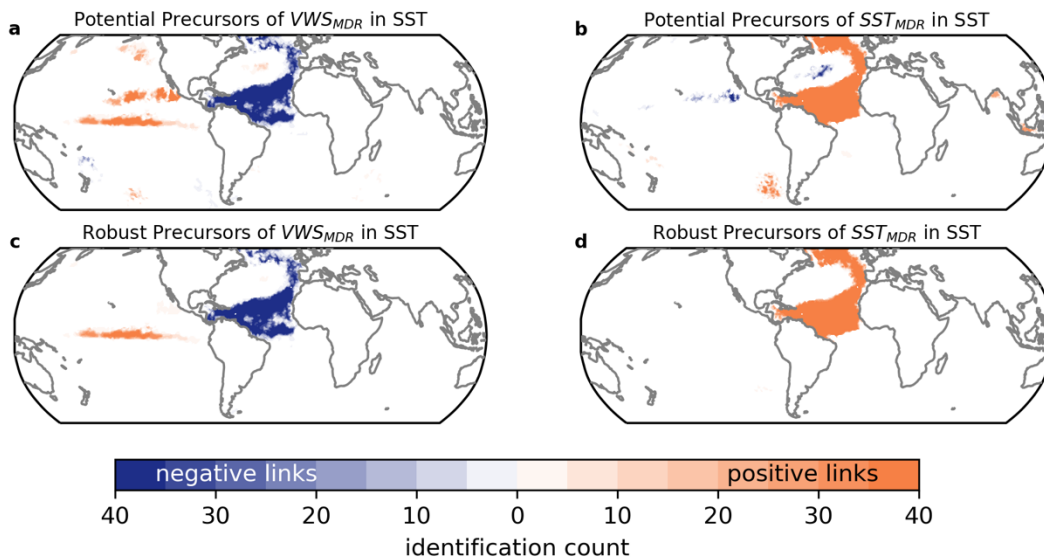


155 **Figure 3: Precursors of  $VWS_{MDR}$  in a training set containing the years 1979-2015: a: Pointwise correlation between SSTs in May and  $VWS_{MDR}$  averaged over July-October. Labels indicate clustered regions that are treated as potential precursors. b: Detected robust precursors of  $VWS_{MDR}$ . The color of the nodes indicates the strength of the auto dependence, the color of the arrows indicates the link strength. Only ingoing links of  $VWS_{MDR}$  are shown here, the full network is shown in Fig. S1.**

160 The correlation maps vary for the different training sets, partly leading to different potential precursors (Fig. 4a-b). For instance, a few regions are not identified as potential precursors in all training sets (lighter shading). Nevertheless, throughout all different training sets, SSTs in the Atlantic and in the Niño3.4 region are consistently identified as robust precursors of  $VWS_{MDR}$  (Fig. 4c).



165 A robust precursor for warm  $SST_{MDR}$  in July-October is a large SST region in the North Atlantic (Fig. 4d). This region extends  
to the north-eastern Atlantic. The strong link of this precursor to  $SST_{MDR}$  is a result of the high autocorrelation of SSTs.  
Furthermore it is likely, that water from north of the MDR would be advected into it during the following months (Klotzbach  
2019). The identified SST signals north in the subpolar Atlantic and Arctic ocean may not have a direct impact on the cyclone  
activity, but could also be the result of the presence of a common driver of multi-month/annual SST in the North Atlantic that  
cannot be resolved by our temporally limited application of the CEN method for forecasting purposes. This does not mean that  
170 the SST signal in the region does not have skill as a robust precursor, but only that no direct ‘causal’ pathway might be at play  
here.



175 **Figure 4: Potential and robust precursors of  $VWS_{MDR}$  and  $SST_{MDR}$  in May. Number of training sets in which a grid-cell is part of a potential (a-b) and robust (c-d) precursor region. The maximum number is 40 - the number of different training sets considered.**

### 3.1 Forecast model based on May precursors

180 We next predict each years’ ACE in July-October with a linear regression model (step 4 in fig. 1) that is based on the absolute values of the robust precursors identified in May for the training set (containing again all years but the predicted year and the two preceding years) (see Fig. 5). With a Pearson correlation coefficient of  $\rho = 0.47$  (and a Spearman rank correlation coefficient of  $\rho_{rank} = 0.53$ ), our cross-validated forecast seems competitive with operational forecasts which have  $\rho < 0.4$  (Klotzbach 2019).

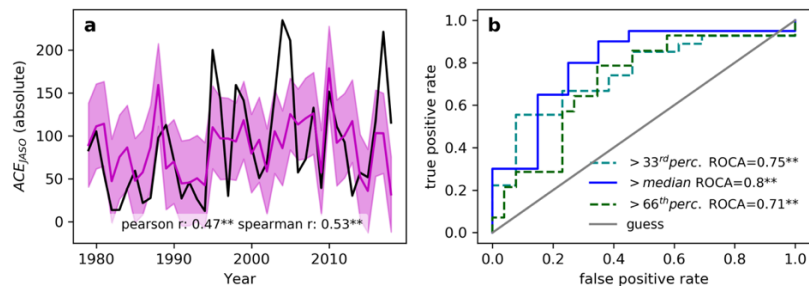


Our model skillfully discriminates between above and below median seasonal activity (Fig. 5b). However, the intensity of most extreme hurricane seasons is underestimated in our linear prediction model (e.g. years 1995, 2004, 2005, 2017 in Fig. 5a). Figure 5b shows that despite this lack in sensitivity of the linear model, it can still deliver valuable information on the occurrence of above 66<sup>th</sup> percentile seasons.

As an addition to the linear model, we next use a logistic regression classifier to construct probabilistic forecast models. We focus on predicting the most active (above 66<sup>th</sup> percentile) and least active (below 33<sup>th</sup> percentile) seasons using the same predictors as for the linear model (Fig. 6b-c). For each year this model gives a probability of having an above 66<sup>th</sup> (below 33<sup>rd</sup>) percentile season. As it does not assume a linear relationship between predictors and predictands it might be more suited for the prediction of extreme seasons.

We evaluate the performance of the model using the Brier skill score (BSS) (Brier 1950). With a positive BSS, the result of the forecast model that gives the probability of finding an above 66<sup>th</sup> percentile season (Fig. 6c) is slightly superior to a climatological forecast, which would be forecasting above 66<sup>th</sup> percentile seasons with a probability of 33% in each year. The usefulness of this forecast is however limited as the reliability curve flattens out for high forecast probabilities. For instance, even when the model predicts an active season with a probability higher than 60%, roughly half of these seasons will be false positives. It rather predicts seasons that are very unlikely to become particularly active with high confidence.

We hypothesise that the deficit to predict some of the most active seasons (e.g. 1995, 2004, 2005 and 2017 compare Fig. 5a) might be due to missing relevant predictors. Klotzbach et al. (2018) argue that the extreme TC activity in 2017 was due to an enhanced Pacific Walker circulation during near neutral ENSO conditions. The Pacific Walker circulation and ENSO are strongly correlated, but in 2017 forecast models using ENSO as an predictor (rather than the Walker circulation) heavily underestimated the seasonal activity (Klotzbach et al. 2018).

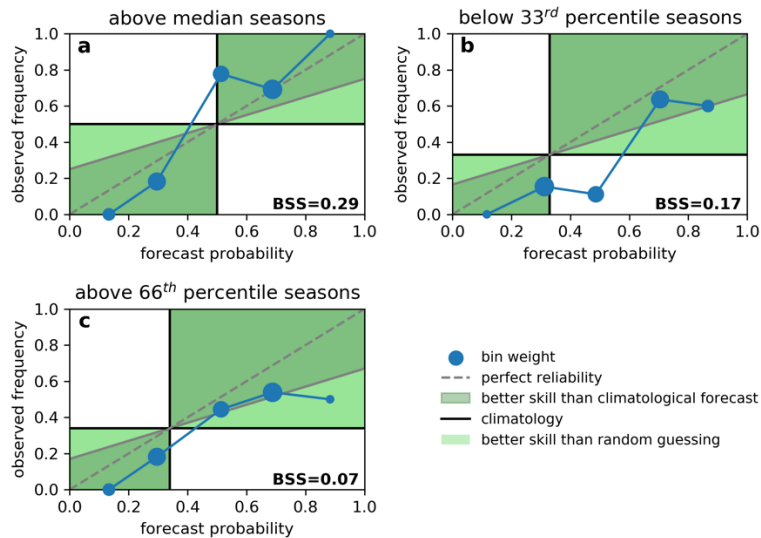


205

**Figure 5: Forecast skill based on May reanalysis. a: ACE yearly aggregated over July-October (black) and based on our linear forecast model using precursors identified for the month of May (magenta). The shading corresponds to a 66% confidence interval based on the standard deviation of the model over the training period. b: Receiver operating characteristic (ROC) curve (see SI) for different seasonal activities: above (the long-term) median seasons in blue, above the 33<sup>rd</sup> percentile in cyan and above the 66<sup>th</sup> percentile in green. The area under the ROC curve (ROCA) is indicated in the legend with significance levels (\*\* - alpha=0.05, \* - alpha=0.1).**

210





215 **Figure 6: Reliability diagrams for a logistic regression model on May reanalysis and for three types of seasonal activities: above median (a), below 33<sup>rd</sup> percentile (b), above 66<sup>th</sup> percentile (c) seasons. Dots show the mean predicted probability versus the observed frequency of a (seasonal) event. The size of the dots indicates the relative amount of data points that contributed to a bin. A perfectly reliable forecast would lie on the diagonal (dashed gray line). Dots within the dark-green area contribute to a forecast skill improvement compared to the climatology while dots within the light-green area contribute to a forecast skill improvement compared to random guessing. The Brier Skill Score (BSS) is indicated in the lower left corner of each panel.**

220

### 3.2 Forecasting at longer lead times

We next apply the same methods to construct a forecast model based on *March* reanalysis data, where existing operational forecasts show little skill (Klotzbach et al. 2017; Klotzbach 2019). Here we find different precursors for VWS<sub>MDR</sub>. At the end of March, it is difficult to forecast the state of ENSO for the upcoming hurricane season due to the ENSO predictability barrier (Torrence and Webster 1998; Hendon et al. 2009). Indeed, in March, the El Niño region is not identified as a robust precursor of VWS<sub>MDR</sub> in July-October (see Fig. S2).

225 We therefore search for robust precursors in mean sea level pressure (MSLP). To avoid spurious effects at this long-time lag on atmospheric time scales, we adjust our criteria to yield large-scale precursors for this atmospheric variable. We therefore cluster the 7.5% most significantly correlated grid cells (instead of 5% elsewhere) into broader precursor regions (all clustering parameters are listed in the SI).

230

Potential precursor regions are identified all over the globe (Fig 7a). As robust precursors, a high-pressure system over the southern Indian Ocean and a low-pressure system eastward of New Zealand are identified in nearly all training sets (Fig 7b).



235

For SSTMDR, autocorrelation still plays an important role and, as for the May forecast, a larger area in the North Atlantic remains a robust predictor (see Fig 7c and d).

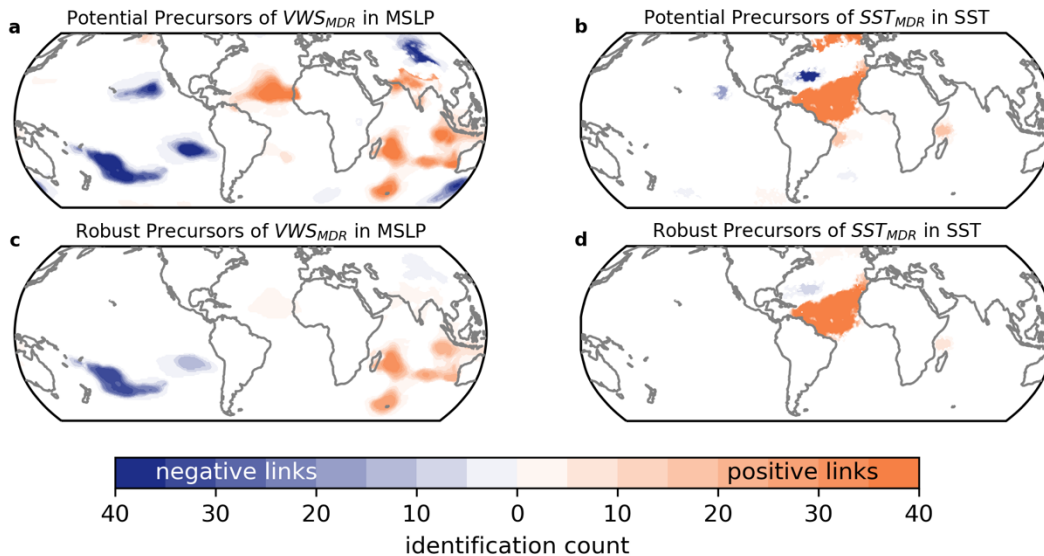


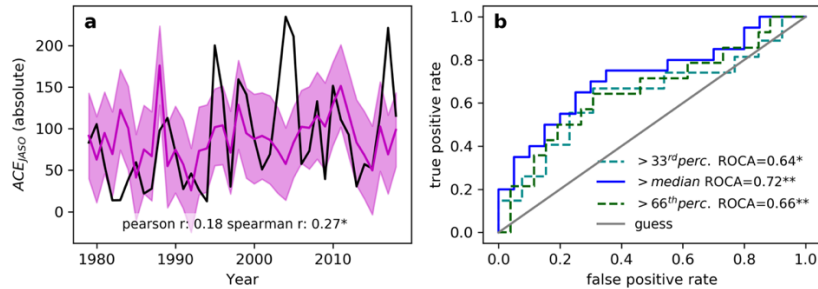
**Figure 7: Potential and robust precursors of  $VWS_{MDR}$  and  $SST_{MDR}$  in March. As Figure 4 but in March and with MSLP precursors for  $VWS_{MDR}$ .**

240 As expected, the overall skill of a forecast based on these March precursors is lower than for the May forecast but still  
considerable with a spearman rank correlation of 0.27 between the observed and the predicted ACE (Fig. 8). Although  
relatively low, this correlation is promising since this correlation is near zero in most operational forecast models (compare  
Klotzbach et al. 2017; Klotzbach 2019).

The linear model shows skill in forecasting above median as well as extremely active seasons (Fig. 8b). For instance an above  
245 66<sup>th</sup> percentile season can be forecasted with a true positive rate of 65% and a false positive rate of 27%.

The forecasts of the logistic regression model for above 66<sup>th</sup> percentile seasons has skill over a climatological forecast ( $BSS =$   
0.11). The reliability diagram (Fig. 9c) shows a rather flat curve with few data points with high observed frequencies. This  
means that when the model predicts high probabilities for above 66<sup>th</sup> percentile seasons a relatively high number of these events  
are false positives. For above median TC activity the reliability curve is substantially closer to the diagonal and the skill over  
250 a climatological forecast is higher ( $BSS = 0.17$  Fig. 9a).

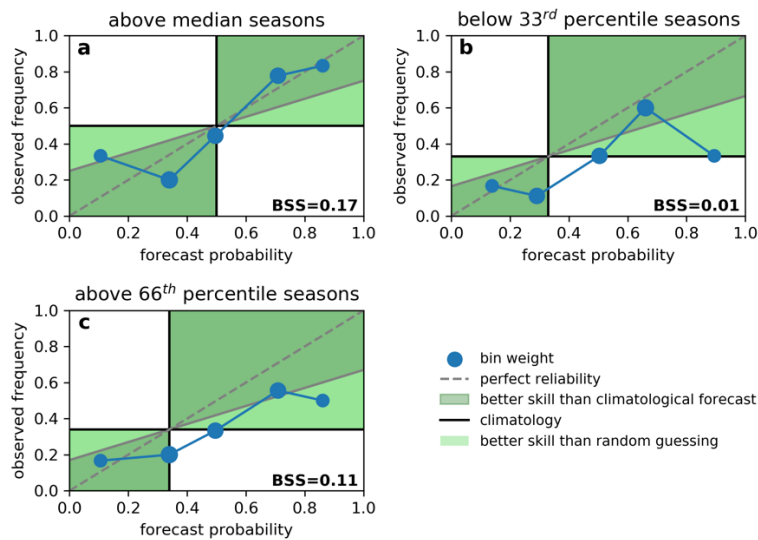
The skill of the March forecast significantly drops when detrended ACE anomalies are predicted using detrended precursor  
anomalies (see Fig. S3). This suggests that the skill of the March forecast model is partly due to the increase in ACE and the  
increase in Atlantic SSTs over the period 1979-2018.



255 **Figure 8: Forecast skill based on March reanalysis. as Figure 5 but for March.**

Since a theoretical explanation of the MSLP dipole pattern is not available as yet, we assessed the relevance of its contribution by constructing a model solely based on SSTs in the Atlantic. This model, however, has no skill (see Fig. S4). Therefore, we can conclude that skill of our forecast model relies on the combination of warm SSTs in the Atlantic and the identified MSLP dipole pattern between the south Indian Ocean and the south Pacific underscoring the relevance of this potential mechanism.

260 The results of our forecast models are to some extent sensitive to the used reanalysis data. Applying the same method to the JRA55 reanalysis results in similar precursors in May and March (Fig. S5-6). Overall these precursors seem less robust in JRA55 and thereby the forecast skill is also slightly reduced (Fig. S7-8).



265

**Figure 9: Reliability diagrams for a logistic regression model on March reanalysis. As Figure 6 but for March.**



270 The reason for this difference might lie in the method applied to identify potential precursors (step 2 in Fig. 1). Applying the same clustering algorithm with the same parameters on a dataset with a different grid size leads to a minimally different clustering behavior and might therefore affect the whole model building approach. This highlights a potential caveat of the method: the strong influence of the clustering step on the identified potential precursors and all the subsequent steps in the analysis.

#### 4 Discussion

275 A crucial component of statistical forecasting is the selection of predictors. Because too many features would lead to overfitting, methods are required to sub-select relevant predictors from a large set of potential predictors (Hawkins 2004). Here we show that causal effect networks can be used to identify a core set of robust predictors.

Warm SSTs in the Atlantic and La Niña conditions in May are identified as robust precursors of active hurricane seasons in July-October. The skill of our forecast model compares well to operational forecast models (Klotzbach 2019), although, the  
280 real forecasting skill of our model can only be evaluated in the coming years.

At longer lead times, the skill of operational forecast models issued at the beginning of April is limited (Klotzbach 2019). Our model based on Atlantic SSTs and two mean sea level pressure regions in the southern Indian Ocean and east of New Zealand in March seems to overcome this forecast barrier and provides valuable predictions of above median and above 66<sup>th</sup> percentile seasonal activity. This forecast seems not to rely on the ENSO signal but on a teleconnection between the identified pressure  
285 regions and vertical wind shear (4 months before the season) in the Atlantic that has not been documented so far. Incorporating this new signal into statistical forecasts that use ENSO projections could therefore lead to an improved skill.

In this study we searched for robust precursors of two well-known favorable conditions for TC formation and intensification: warm SSTs and low vertical wind shear in the Atlantic main development region. Including more variables to the characterization of favorable conditions as relative humidity or upper troposphere temperatures could further increase the skill.

290 It might, however, be challenging to incorporate these conditions in our current framework that works on seasonal time scales. We constructed causal effect networks for favorable conditions in the hurricane season and their potential precursors in SSTs or MSLP at a fixed time lag of 2 or 4 months. In our application, the underlying assumptions of the causal effect network algorithm are not strictly fulfilled (Runge 2018) and thus we cannot guarantee that the identified links are “truly causal”. The causal effect network rather helps to identify “the least spuriously link” and therefore most robust precursors or most skillful  
295 predictors.

A challenge that we did not address here are potential non-stationarities in the climate system. The detected causal links might not be stationary over time, which could lead to varying forecast skill. Unfortunately, the time span for which reliable reanalysis datasets exists is limited which makes further investigation of this problem challenging. One way to deal with this is to apply this approach to climate simulations for which longer time series are available.



300 The forecast model construction technique developed in this study is highly automated and can easily be applied for seasonal  
forecasts of other meteorological phenomena. In our view the most critical step in the approach is the identification of potential  
precursors (step 2 in fig. 1). Depending on the free parameters of the clustering algorithm and significance threshold for  
correlated grid-cells, the detected potential precursor regions can vary and subsequently affect the causal network. Improving  
the robustness of this step or finding alternative ways of defining these potential precursors would further enhance the  
305 applicability of the method.

#### 4 Conclusions

We applied causal effect networks to identify skillful predictors for seasonal Atlantic hurricane forecasts. For shorter lead  
times we identify well known precursors while for longer lead times we find novel predictors from which a competitive early  
April forecast model can be constructed. Our model shows competitive skill in forecasting seasonal hurricane activity, although  
310 some challenges in the representation of the most active hurricane seasons remain.

We see different entry points for our findings to be incorporated into applied seasonal hurricane forecasts. Besides a direct  
application of our early April forecast model we encourage other statistical forecasting groups to investigate whether our newly  
identified predictors can help to improve their statistical forecast models. Furthermore, the causal links identified here could  
be a basis for hybrid forecasting techniques where a dynamical forecast ensemble is constrained by selecting only members  
315 that adequately reproduce the causal links as demonstrated by Dobrynin et al. (2018).

Improved seasonal forecasting with long lead-times can support seasonal planning of disaster risk reduction measures,  
particularly also related to disaster relief and emergency aid provision. While basin scale dissipated energy does not directly  
provide risk profiles for individual countries, it however allows to inform decision making on the regional level, including on  
financial support needs pooled e.g. in the Caribbean Catastrophe Risk Insurance Facility serving Caribbean islands states. As  
320 such, improved seasonal forecasting can provide essential information to ensure hurricane preparedness in affected countries.



### Code availability

All python scripts required to reproduce the analysis are available under:

325 [github.com/peterpeterp/atlantic\\_ace\\_seasonal\\_forecast](https://github.com/peterpeterp/atlantic_ace_seasonal_forecast)

### Author contributions

P.P., C.-F.S., T.G. and M.K. conceived the study. P.P. did the analysis and created all figures. P.P. wrote the manuscript with contributions from all authors.

### Competing interests

330 The authors declare no competing interests.

### References

- Brier GW (1950) Verification of forecasts expressed in terms of probability. *Mon Weather Rev* 78:1–3
- Camargo SJ, Hsiang SM (2014) Tropical Cyclones: From the Influence of Climate to their Socio-Economic Impacts. *Extrem Events Obs Model Econ* 73:90. doi: 10.1002/9781119157052.ch18
- 335 Copernicus Climate Change Service (C3S) (2017) ERA5: Fifth generation of ECMWF atmospheric reanalyses of the global climate. In: Copernicus Clim. Chang. Serv. Clim. Data Store. <https://cds.climate.copernicus.eu/cdsapp#!/home>. Accessed 12 Nov 2019
- Di Capua G, Kretschmer M, Runge J, et al (2019) Long-lead statistical forecasts of the indian summer monsoon rainfall based on causal precursors. *Weather Forecast* 34:1377–1394. doi: 10.1175/WAF-D-19-0002.1
- 340 Dieng AL, Sall SM, Eymard L, et al (2017) Trains of African Easterly Waves and Their Relationship to Tropical Cyclone Genesis in the Eastern Atlantic. *Mon Weather Rev* 145:599–616. doi: 10.1175/MWR-D-15-0277.1
- Dobrynin M, Domeisen DI V., Müller WA, et al (2018) Improved Teleconnection-Based Dynamical Seasonal Predictions of Boreal Winter. *Geophys Res Lett* 45:3605–3614. doi: 10.1002/2018GL077209
- Emanuel K, DesAutels C, Holloway C, Korty R (2004) Environmental Control of Tropical Cyclone Intensity. *J Atmos Sci* 61:843–858. doi: 10.1175/1520-0469(2004)061<0843:ECOTCI>2.0.CO;2
- 345 Frank WM, Ritchie EA (2001) Effects of vertical wind shear on the intensity and structure of numerically simulated hurricanes. *Mon Weather Rev* 129:2249–2269. doi: 10.1175/1520-0493(2001)129<2249:EOVWSO>2.0.CO;2
- Gray WM (1984a) Atlantic Seasonal Hurricane Frequency. Part I: El Niño and 30 mb Quasi-Biennial Oscillation Influences. *Mon Weather Rev* 112:1649–1668. doi: 10.1175/1520-0493(1984)112<1649:ASHFPI>2.0.CO;2
- 350 Gray WM (1984b) Atlantic Seasonal Hurricane Frequency. Part II: Forecasting its Variability. *Mon Weather Rev* 112:1669–



1683. doi: 10.1175/1520-0493(1984)112<1669:ASHFPI>2.0.CO;2
- Hankes I, Marinaro A (2016) The impacts of column water vapour variability on Atlantic basin tropical cyclone activity. *Q J R Meteorol Soc* 142:3026–3035. doi: 10.1002/qj.2886
- Hawkins DM (2004) The Problem of Overfitting. *J. Chem. Inf. Comput. Sci.* 44:1–12
- 355 Hendon HH, Lim E, Wang G, et al (2009) Prospects for predicting two flavors of El Niño. *Geophys Res Lett* 36:L19713. doi: 10.1029/2009GL040100
- Kim H-M, Webster, PJ, Curry JA (2009) Impact of Shifting Patterns of Pacific Ocean Warming on North Atlantic Tropical Cyclones. *Science* (80- ) 325:77–80. doi: 10.1126/science.1174062
- Klotzbach PJ (2019) Seasonal Tropical Cyclone Forecasting. doi: 10.6057/2019TCRR03.03
- 360 Klotzbach PJ, Saunders MA, Bell GD, Blake ES (2017) North Atlantic Seasonal Hurricane Prediction. pp 315–328
- Klotzbach PJ, Schreck CJ, Collins JM, et al (2018) The extremely active 2017 North Atlantic hurricane season. *Mon Weather Rev* 146:3425–3443. doi: 10.1175/MWR-D-18-0078.1
- Knapp KR, Diamond HJ, Kossin JP, et al (2018) International Best Track Archive for Climate Stewardship (IBTrACS) Project, Version 4. In: NOAA Natl. Centers Environ. Information. <https://doi.org/10.25921/82ty-9e16>. Accessed 26 Sep 2019
- 365 Knapp KR, Kruk MC, Levinson DH, et al (2010) The international best track archive for climate stewardship (IBTrACS). *Bull Am Meteorol Soc* 91:363–376. doi: 10.1175/2009BAMS2755.1
- Kretschmer M, Coumou D, Donges JF, Runge J (2016) Using Causal Effect Networks to analyze different Arctic drivers of mid-latitude winter circulation. *J Clim* 160303130523003. doi: 10.1175/JCLI-D-15-0654.1
- Kretschmer M, Runge J, Coumou D (2017) Early prediction of extreme stratospheric polar vortex states based on causal precursors. *Geophys Res Lett* 44:8592–8600. doi: 10.1002/2017GL074696
- 370 Li J, Liu L, Le TD, Liu J (2020) Accurate data-driven prediction does not mean high reproducibility. *Nat Mach Intell* 2:13–15. doi: 10.1038/s42256-019-0140-2
- Manganello J V., Cash BA, Hodges KI, Kinter JL (2017) Seasonal forecasts of North Atlantic tropical cyclone activity in the North American Multi-Model Ensemble. *Clim Dyn* 0:1–16. doi: 10.1007/s00382-017-3670-5
- 375 Martinez AB (2018) A false sense of security: The impact of forecast uncertainty on hurricane damages. *Univ Oxford, Dep Econ Discuss Pap* 831:. doi: 10.2139/ssrn.3070154
- Murakami H, Levin E, Delworth TL, et al (2018) Dominant effect of relative tropical Atlantic warming on major hurricane occurrence. *Science* (80- ) 6711:eaat6711. doi: 10.1126/science.aat6711
- Patricola CM, Saravanan R, Chang P (2018) The Response of Atlantic Tropical Cyclones to Suppression of African Easterly Waves. *Geophys Res Lett* 45:471–479. doi: 10.1002/2017GL076081
- 380 Runge J (2018) Causal network reconstruction from time series: From theoretical assumptions to practical estimation. *Chaos* 28:. doi: 10.1063/1.5025050
- Runge J (2014) TIGRAMITE – Causal discovery for time series datasets. GitHub Repos.
- Runge J, Bathiany S, Bollt E, et al (2019a) Inferring causation from time series in Earth system sciences. *Nat Commun* 10:2553.



- 385        doi: 10.1038/s41467-019-10105-3
- Runge J, Nowack P, Kretschmer M, et al (2019b) Detecting and quantifying causal associations in large nonlinear time series datasets. *Sci Adv* 5:eaa4996. doi: 10.1126/sciadv.aau4996
- Saggioro E, Shepherd TG (2019) Quantifying the timescale and strength of Southern Hemisphere intra-seasonal stratosphere-troposphere coupling. *Geophys Res Lett*. doi: 10.1029/2019gl084763
- 390    Tang BH, Neelin JD (2004) ENSO Influence on Atlantic hurricanes via tropospheric warming. *Geophys Res Lett* 31:L24204. doi: 10.1029/2004GL021072
- The Japan Meteorological Agency (JMA) (2013) JRA-55: Japanese 55-year Reanalysis, Daily 3-Hourly and 6-Hourly Data
- Torrence C, Webster PJ (1998) The annual cycle of persistence in the El Niño/Southern Oscillation. *Q J R Meteorol Soc* 124:1985–2004. doi: 10.1256/smsqj.55009
- 395    Vecchi GA, Delworth T, Gudgel R, et al (2014) On the seasonal forecasting of regional tropical cyclone activity. *J Clim* 27:7994–8016. doi: 10.1175/JCLI-D-14-00158.1
- Vecchi GA, Soden BJ (2007) Effect of remote sea surface temperature change on tropical cyclone potential intensity. *Nature* 450:1066–1070. doi: 10.1038/nature06423
- Vitart F, Stockdale TN (2001) Seasonal forecasting of tropical storms using coupled GCM integrations. *Mon Weather Rev* 129:2521–2537. doi: 10.1175/1520-0493(2001)129<2521:SFOTSU>2.0.CO;2
- 400    Waple AM, Lawrimore JH, Halpert MS, et al (2002) CLIMATE ASSESSMENT FOR 2001. *Bull Am Meteorol Soc* 83:S1--S62
- Woodruff JD, Irish JL, Camargo SJ (2013) Coastal flooding by tropical cyclones and sea-level rise. *Nature* 504:44–52. doi: 10.1038/nature12855
- 405    Ye Y, Fang W (2018) Estimation of the compound hazard severity of tropical cyclones over coastal China during 1949–2011 with copula function. *Nat Hazards* 93:887–903. doi: 10.1007/s11069-018-3329-5